Spin-parity analysis of $\bar{p}p \rightarrow E(1420)X$

D. F. Reeves, D. Boehnlein, J. H. Goldman, and V. Hagopian
Florida State University, Tallahassee, Florida 32306

S. U. Chung, R. C. Fernow, H. Kirk, S. D. Protopopescu, and D. P. Weygand
Brookhaven National Laboratory, Upton, New York 11973

R. Crittenden, A. Dzierba, T. Marshall, S. Teige, and D. Zieminska
Indiana University, Bloomington, Indiana 47401

Z. Bar-Yam, J. Dowd, W. Kern, and H. Rudnicka
Southeastern Massachusetts University, N. Dartmouth, Massachusetts 02747
(Received 3 January 1986)

A Dalitz-plot analysis of 620 $E(1420)$ events was performed on the reaction $\bar{p}p \rightarrow (K_S^0 K^+ \pi^-)X$ at 6.6 GeV/c, obtained at the Brookhaven National Laboratory Multiparticle Spectrometer facility. The mass and width of the $E(1420)$ peak are 1424 ± 3 and 60 ± 10 MeV, respectively. The best fit to the $E(1420)$ is a $J^{PG}=0^{-+}$ state with a substantial $\delta\pi$ decay mode, produced over a large nonresonant background of 1^{++} K^*K and phase space. This fit shows the same characteristics as the $E(1420)$ observed in our companion $\pi^- p$ experiment.

A Dalitz-plot analysis was performed on the $K\bar{K}\pi$ system in the mass range 1.32—1.60 GeV. The data were produced by the reaction

$$\bar{p}p \rightarrow (K_S^0 K^+ \pi^-)X \text{ at 6.6 GeV}/c \ , \quad (1)$$

where X represents missing particles. In this mass range two peaks $D(1285)$ and $E/\iota(1420-1460)$ are observed which decay to $K\bar{K}\pi$. The procedure that was used to determine the J^{PC} (spin-parity, C parity) is the same as that used in our previously reported analysis[1] of the reaction

$$\pi^- p \rightarrow (K_S^0 K^+ \pi^-)n \text{ at 8.0 GeV}/c \ . \quad (2)$$

The $E(1420)$ was first observed in 1963 by Armenteros *et al.*[2] The first systematic study of the J^{PC} and decay modes of about 800 events obtained in $\bar{p}p$ annihilation at rest was performed by Baillon *et al.*,[3] with the determination that $J^{PC}=0^{-+}$. A later reanalysis using maximum likelihood on the same data[4] confirmed the J^{PC} assignment. In 1980 Dionisi *et al.*[5] observed in $\pi^- p \rightarrow K_S^0 K^{\pm}\pi^{\mp} n$ a bump at the same mass with about 150 events, but determined $J^{PC}=1^{++}$. Since then several other hadron-production experiments have also observed peaks at the same mass with J^{PC} determinations of either 0^{-+} (Ref. 6) or 1^{++} (Ref. 7). Interest in this peak increased when a broader resonance was observed by several groups in the radiative decay of the J/ψ with a mass of 1440—1460 MeV.[8] The spin-parity of this object was determined to be 0^{-+}. Since the Particle Data Group[9] had already listed the $E(1420)$ as 1^{++}, this peak from radiative decay $J/\psi \rightarrow (K\bar{K}\pi)\gamma$ was named the $\iota(1440)$. It is perhaps noteworthy that all the hadron-production experiments observe the E peak at a mass within 5 MeV of 1421 MeV, while the ι peak is between 1440 and 1460 MeV depending on cuts.

A high-statistics experiment to study this E/ι region was performed at the Brookhaven National Laboratory Multiparticle Spectrometer (MPS) facility using both π^- and $\bar{p}$ beams. Analysis of the π^--beam results on 2000 $E(1420)$ events has been reported[1] and preliminary results of the $\bar{p}$-beam data have been reported at several conferences.[10]

The experimental apparatus and analysis method used for the $\bar{p}p$ data are discussed in more detail in Ref. 11. The experimental layout is shown in Fig. 1. The MPS

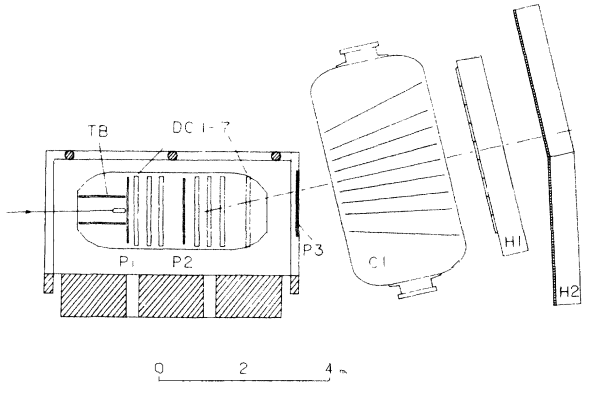

FIG. 1. Experimental apparatus. The arrow points to the 60-cm liquid-hydrogen target, surrounded by a scintillator box (TB). $P1$—$P3$ are proportional wire chambers; DC1—DC7 are drift chamber modules; $H1$,$H2$ are scintillator-counter hodoscopes; $C1$ is a high-pressure Cherenkov counter.

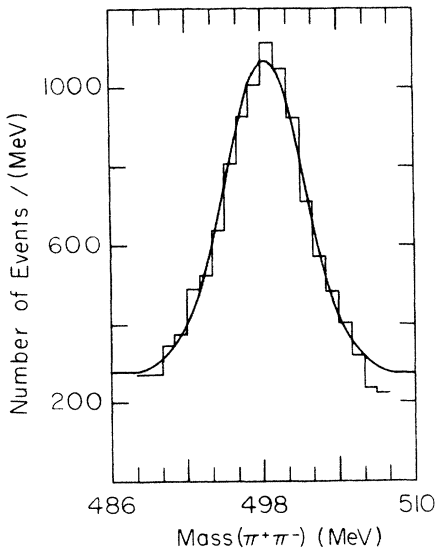

FIG. 2. $\pi^+\pi^-$ mass spectrum for the decay vertex. Curve is fitted with Gaussian and flat background, giving a K_S^0 mass of 498±1 MeV.

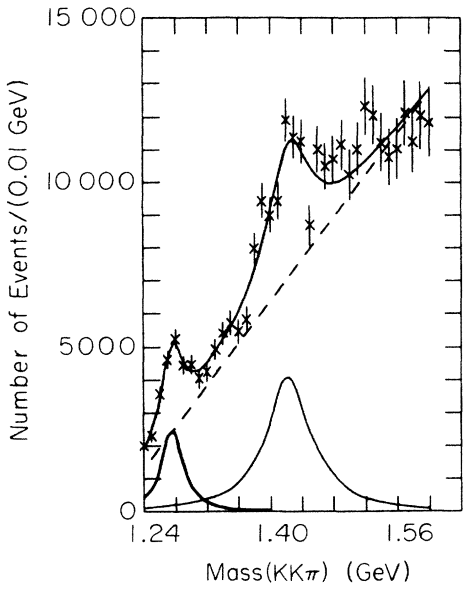

FIG. 4. $K^+K_S^0\pi^-$ mass spectrum corrected for acceptance. Top curve is a fit with two Breit-Wigner functions for the D and the E plus a polynomial background. Mass and width of D is 1277±2 and 32±8 MeV; that of E is 1424±3 and 60±10 MeV. Dashed line is background; bottom curves are the two Breit-Wigner functions.

facility consists of seven drift-chamber modules (DC1–DC7) with seven planes each,[12] plus three proportional wire chambers ($P1$, $P2$, $P3$) interspersed, all within the MPS magnet, with the field set at 0.5 T. Downstream of the magnet were the Cherenkov counter ($C1$), set at $\gamma_{\text{threshold}}=10$, and two scintillator hodoscopes ($H1$, $H2$). The liquid-hydrogen target was 60 cm long (compared to 30 cm for the π^- run) and was surrounded by a scintillator target box (TB). The trigger consisted of a fast-forward K^+ or p and a multiplicity requirement to enrich the sample with V's, which decay to charged particles. The fast-forward K^+ or p selection was made by two independent coincidence matrices: $P2\times P3\times H2$ for momentum determination and $P2\times P3\times(H1\cdot\bar{C}\,\bar{1})$ for particle identification. For this data the momentum selection was at ≥ 1.5 GeV/c with a corresponding Cherenkov cell ($C1$) in veto mode. In addition, the multiplicity was ≥ 2 in $P1$ and ≥ 4 in $P2$. (For the π^- beam experiment the multiplicity requirement was exactly 2 in $P1$ and exactly 4 in $P2$.) The efficiency of the high-pressure Cherenkov counter $C1$ was above 99% for pions of momenta above 1.5 GeV/c.

The $\bar{p}$ beam at 6.6 GeV/c was electrostatically separated and also identified by the veto of three Cherenkov

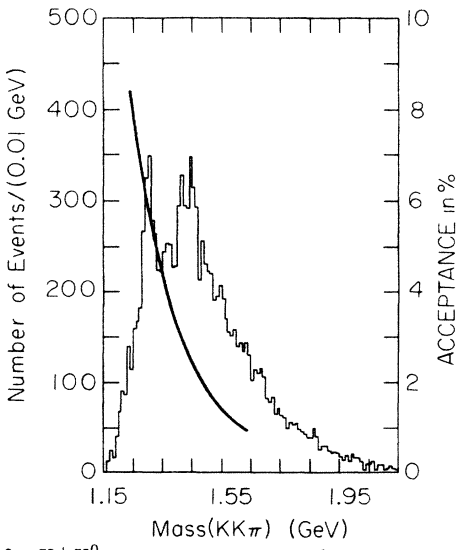

FIG. 3. $K^+K_S^0\pi^-$ mass spectrum and acceptance curve.

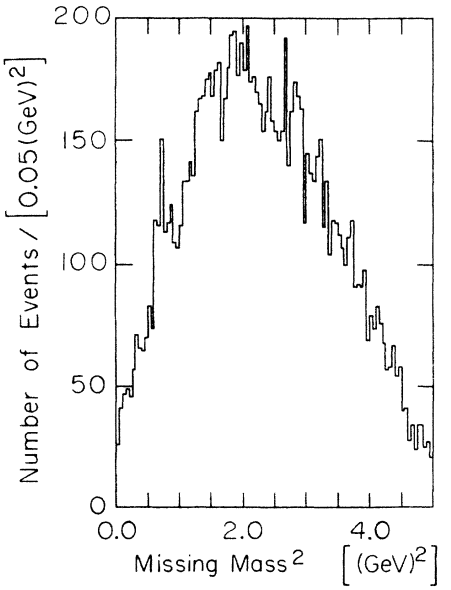

FIG. 5. Missing mass squared (X) in $\bar{p}p \to (K^+K_S^0\pi^-)X$.

counters. On the average about 100 000 $\bar{p}$'s reached the hydrogen target per pulse. The efficiency of tagging the $\bar{p}$'s was better than 99%, but the beam had a misidentified π^- contamination of a few percent. The integrated beam flux was 19×10^9 $\bar{p}$ particles with a beam momentum spread of 1.5%.

About 5×10^6 triggers were recorded on tape. Topology selection, K_S^0 mass cut, and a $-0.2\le t\le 1.2$ $(\mathrm{GeV}/c^2)^2$ cut, where t is the momentum transfer squared from the $\bar{p}$ to the $(K_S^0K^+\pi^-)$ system, yielded a data sample of about 12 000 events. The K_S^0 mass spectrum is shown in Fig. 2; a Gaussian function plus flat background fit gave a mass of 498 ± 1 MeV. The uncorrected $K_S^0K^+\pi^-$ mass spectrum is shown in Fig. 3. Our estimate of the mass resolution (σ) in the $E(1420)$ region is 10 MeV. The acceptance of $K^+K_S^0\pi^-$ events is also shown in Fig. 3 and falls rapidly with mass. It is about 6% at the $D(1285)$ and 3% at the $E(1420)$. The acceptance has three parts: first, about 45% of the K^+'s decay before reaching the end of the apparatus (i.e., H2 shown in Fig. 1, which is part of the trigger); second, to select the $K_S^0\to\pi^+\pi^-$, the K_S^0 vertex was required to be separated from the primary vertex by ≥3.0 cm, corresponding to a loss of another 45% of the events; third, geometrically all the pions were required to travel to at least $P2$ (Fig. 1) and the K^+ all the way to $H2$ at the end of the apparatus. Monte Carlo simulation of events traversing through the equipment showed the acceptance to vary less than 10% over a Dalitz-plot surface in the variables of square of mass of $K_S^0\pi^-$ and $K^+\pi^-$. Monte Carlo simulation, including track-reconstruction efficiency, showed that the event-reconstruction failure rate to be very small (there are 49 drift-chamber planes), and the overall reconstruction efficiency to be above 95% and insensitive to event topology. The inefficiencies of the trigger elements were determined to be independent of event topology and $K\bar{K}\pi$ mass. The mass spectrum corrected for acceptance, shown in Fig. 4, was fitted to two Breit-Wigner functions and a polynomial background. For the $D(1285)$, the fit gave a mass and width of 1277 ± 2 and 32 ± 8 MeV, and for the $E(1420)$, 1424 ± 3 and 60 ± 10 MeV. The D and E peaks, before acceptance correction, correspond to 420 ± 40 and 620 ± 50 events, respectively, within one full width of maximum. The non-$K^+K_S^0\pi^-$ background under the peaks come from three sources. The largest source is misidentified K^+'s. The Cherenkov counter $C1$ in Fig. 1 eliminates π^+'s with better than 99% efficiency, but cannot differentiate a K^+ from a proton. Second, about 25% of the K_S^0 signal is accidental $\pi^+\pi^-$ combinations that come close to the K^0 mass. Third, some $\bar{p}$'s are mislabeled as π^-'s. Fortunately, the non-$K^+K_S^0\pi^-$ background does not interfere with the real events and merely creates a background which is parametrized by a simple phase-space function. Some of the events under the peak are real $K^+K_S^0\pi^-$ events, but

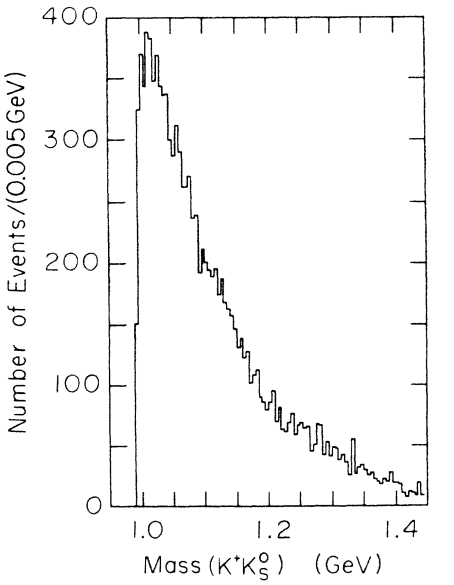

FIG. 6. $K^+K_S^0$ mass, uncorrected for acceptance.

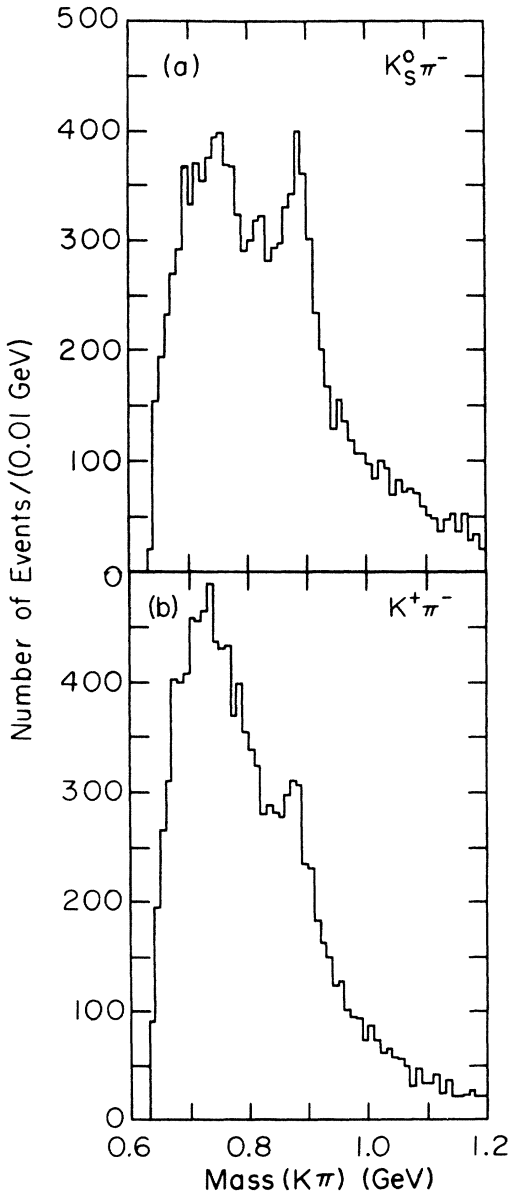

FIG. 7. $K\pi$ masses, uncorrected for acceptance.

the exact proportion cannot be determined.

The distribution of the square of the missing mass (namely, the mass of X in $\bar{p}p \to K^+K_S^0\pi^-X$) is shown in Fig. 5. It displays only one significant structure. The peak between 0.5 and 1.0 GeV^2 is most likely the $\rho \to \pi^+\pi^-$. A ρ cut was applied and the resulting $KK\pi$ mass spectrum showed both the D and E, but with statistics so reduced that an analysis was not possible. The usual production quantity distributions (rapidity, breakup angle, transverse and longitudinal momentum) are consistent with annihilation production.

Figures 6 and 7 show the intermediate states, $K_S^0K^+$, $K_S^0\pi^-$, and $K^+\pi^-$. The steep threshold enhancement of KK in Fig. 6 is identified as the $\delta \to K_S^0K^+$. The peaks at 890 MeV in Fig. 7 are $K^* \to K\pi$.

In this experiment only the G parity can be determined. Since both the D and the E/ι are known to have isotopic spin $I=0$, then the charge-conjugation parity C is equal to the G parity, i.e., $C=G$. Nevertheless, the notation of J^{PG} instead of J^{PC} will be used for the remainder of this paper. A mass-independent Dalitz-plot analysis was performed to determine the J^{PG} of the $D(1285)$ and $E(1420)$. The Zemach amplitudes[13] were used to represent the different J^{PG} waves. The isobar model was used with two intermediate states: $\delta\pi$, $\delta \to K\bar{K}$ for both the D and E, and, in addition, K^*K, $K^* \to K\pi$ for the E. The δ was parametrized as given by Flatte[14] (and used by Dionisi *et al.*[5] and Chung *et al.*[1]) and the K^* was parametrized by a conventional Breit-Wigner function.

Considering only $l=0,1$ and $J=0,1$ waves, two $K\bar{K}\pi$

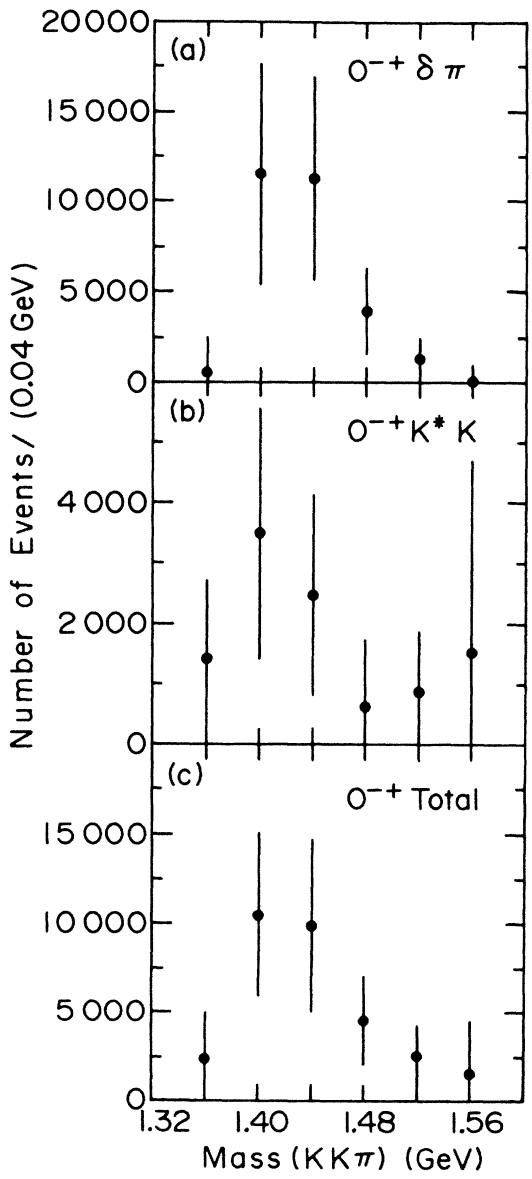

FIG. 8. Results of Dalitz-plot analysis of $J^{PG}=0^{-+}$ waves.

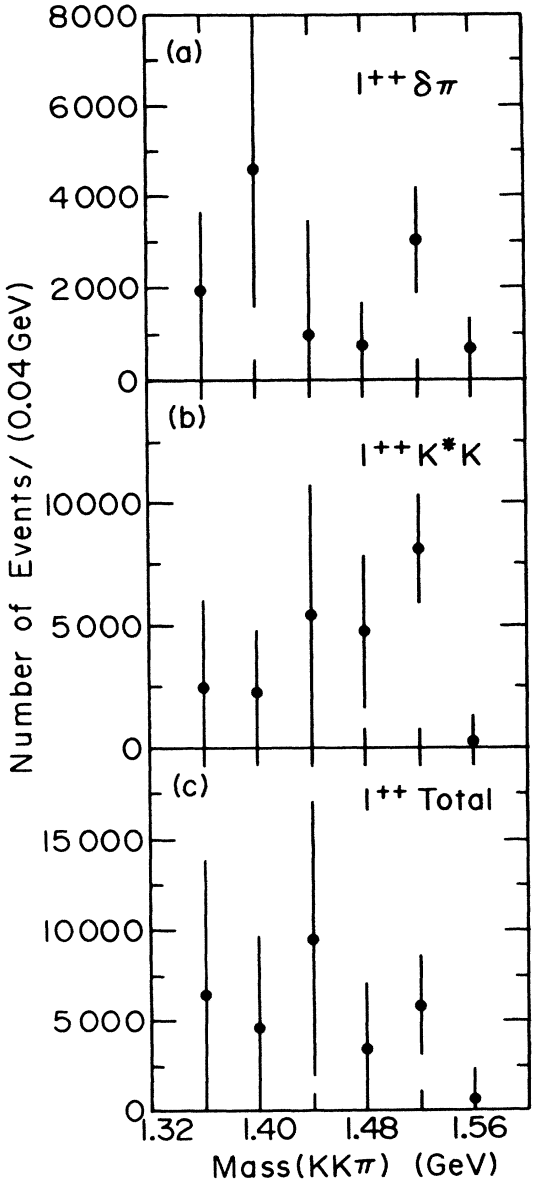

FIG. 9. Results of Dalitz-plot analysis of $J^{PG}=1^{++}$ waves.

TABLE I. Parametrizations. $F_{\rm BW}(m)=1/[r^2-m^2-(ir\Gamma)(q_{ab}^m/q_{ab}^r)^{2l+1}]$, where m is the observed mass of system, r the resonance mass, Γ the width at half maximum, q_{ab}^m the breakup momentum of mass m into masses a and b, and l the angular momentum between particles a and b. For the $F_{\rm BW}(\delta)$ we have taken $r=d-\frac{1}{2}g^2(\Gamma_\eta)(\gamma_{K\bar K}^d/q_{\eta\pi}^d)=971$ MeV and $\Gamma=\Gamma_\eta(q_{\eta\pi}^m+g^2q_{K\bar K}^m)/q_{\eta\pi}^d$, where d is the observed resonance mass of δ in $\eta\pi$ data, Γ_η the observed width of δ in $\eta\pi$ data, $\gamma_{K\bar K}^d=(m_K{}^2-\frac{1}{4}d^2)^{1/2}$, m_K is the average mass of K^+/K_S^0, g the ratio of SU(3) coupling coefficients for the decays: $\delta^+\to\bar K{}^0K^+/\delta^+\to\eta\pi^+$. $g^2=\frac{3}{2}$ and $\mathbf{P}(p_1;p_1p_2)$ stands for the momentum of p_1 evaluated in the p_1p_2 rest frame.

Decay l	Mode J^{PG}	Parametrization of amplitude
$\delta\pi$		
0	0^{-+}	$F_{\rm BW}(\delta)$
1	1^{++}	$F_{\rm BW}(\delta)\mathbf{P}(\pi;\delta\pi)$
K^*K		
0	1^{+G}	$F_{\rm BW}(K^{*-})\mathbf{P}(K_S^0;K_S^0\pi^-)+(G)F_{\rm BW}(K^{*0})\mathbf{P}(K^+;K^+\pi^-)$
1	0^{-G}	$F_{\rm BW}(K^{*-})[\mathbf{P}(K_S^0;K_S^0\pi^-)\cdot\mathbf{P}(K^+;K_S^0K^+\pi^-)]$ $+(G)F_{\rm BW}(K^{*0})[\mathbf{P}(K^+;K^+\pi^-)\cdot\mathbf{P}(K_S^0;K_S^0K^+\pi^-)]$
1	1^{-G}	$F_{\rm BW}(K^{*-})[\mathbf{P}(K_S^0;K_S^0\pi^-)\times\mathbf{P}(K^+;K_S^0K^+\pi^-)]$ $+(G)F_{\rm BW}(K^{*0})[\mathbf{P}(K^+;K^+\pi^-)\times\mathbf{P}(K_S^0;K_S^0K^+\pi^-)]$

states are possible for the $D(1285)$, 0^{-+} and 1^{++}, each decaying into $\delta\pi$; eight $K\bar K\pi$ states are possible for the $E(1420)$; 0^{-+} and 1^{++}, each decaying into $\delta\pi$ and K^*K, and 0^{--}, 1^{+-}, 1^{-+}, and 1^{--}, each decaying only into K^*K. Also used were phase-space background and incoherent $\delta\pi$ and K^*K waves. States of the same J^P were allowed to interfere. See Table I for the explicit parametrizations.

A maximum-likelihood analysis was performed with the logarithm of the likelihood given by

$$\ln L=\sum_{i=1}^{n}\ln\frac{F(\rho_i)}{\int F(\rho)A(\rho)d\rho}\ , \tag{3}$$

where $F(\rho)$ is the square of the sum of the J^{PG} amplitudes at the phase space point ρ. $A(\rho)$ is the acceptance of our apparatus, which was calculated using the Monte Carlo simulation discussed before. The acceptance of events of a particular mass varied by less than 10%, independent of whether the production was phase space, $\delta\pi$ decay, or K^*K decay. The results of the analysis of the $D(1285)$ region showed that the assignment of 1^{++} is slightly preferred over 0^{-+}. As seen in Table I, the parametrization of the 0^{-+} $\delta\pi$ and 1^{++} $\delta\pi$ differ only by the $\delta\pi$ breakup momentum. Because the $D(1285)$ is so close to threshold, it has minimal phase space as compared to the $E(1420)$ region and hence the background becomes relatively more significant. Thus, even though the signal-to-background ratios of the $D(1285)$ and $E(1420)$ are about the same, a J^{PG} determination of the $D(1285)$ was not possible by the Dalitz-plot method.

The analysis of the $E(1420)$ region was performed in 40-MeV mass intervals in the $K\bar K\pi$ mass range, 1.32–1.60 GeV. The 0^{--}, 1^{-+}, 1^{--}, and incoherent waves were found not to contribute and were not included in the final fits. The likelihoods of various fits of interest are shown in Table II. The interpretation of the fits is complicated by the fact that there is a large non-$K^+K_S^0\pi^-$ background. Even though phase space should

TABLE II. Comparison of likelihoods, E region. All fits include phase-space background.

Waves in fit	Difference in ln likelihood from best fit 1.34–1.38 (GeV)	1.38–1.42 (GeV)	1.42–1.46 (GeV)	1.46–1.52 (GeV)
0^{-+} 1^{++} 1^{+-}	0	0	0	0
1^{++} 1^{+-}	−6	−10	−7	−5
0^{-+} 1^{++}	−12	−12	−14	−4
0^{-+} 1^{+-}	−12	−13	−19	−6
1^{++}	−14	−20	−25	−13
0^{-+}	−19	−25	−38	−20
1^{+-}	−44	−55	−55	−18
0^{-+} 1^{++} K^*K 1^{+-}	−7	−12	−13	−16
0^{-+} K^*K 1^{++} K^*K		−18	−25	
0^{-+} $\delta\pi$ 1^{++} $\delta\pi$		−70	−66	

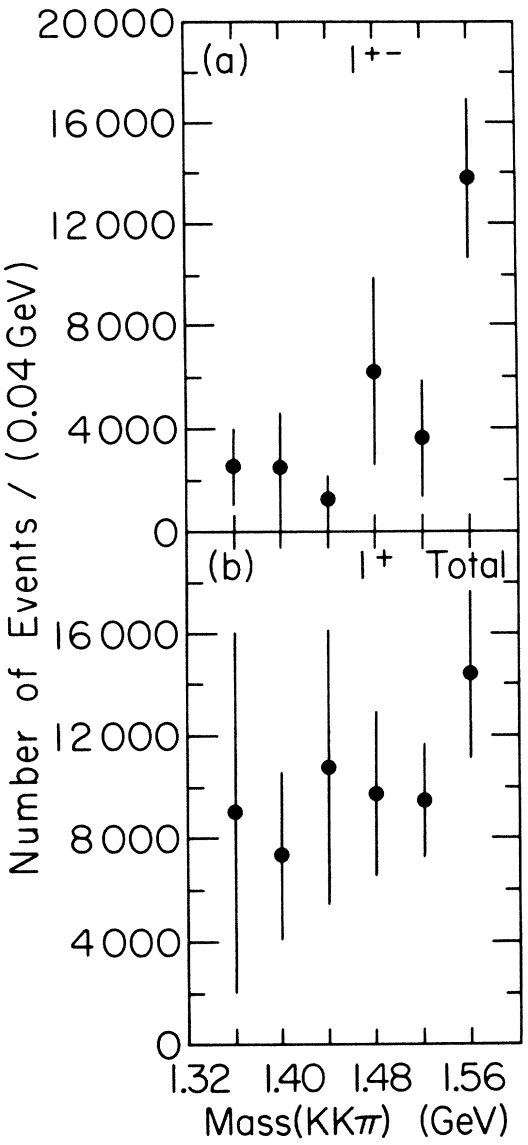

FIG. 10. Results of Dalitz-plot analysis of $J^{PG}=1^{+-}$ and 1^{+} total waves.

describe this background, it can affect the fits, especially when only one J^{PG} is considered. In determining which wave resonates, the important factor is the change across the mass spectrum. When only one wave is fitted, be it 0^{-+}, 1^{++}, or 1^{+-}, that wave will show resonance since the data have a peak at the $E(1420)$ mass. The best fit contained 0^{-+}, 1^{++}, and 1^{+-} waves and a phase-space background. Plots of the results of this fit are shown in Figs. 8–11. Dalitz plots in the $E(1420)$ region of the data and of Monte Carlo–generated events using the parameters of the best fit are shown in Fig. 12.

The peak at 1420 MeV is well established in our data. The significance is over 10 standard deviations. The mass is too far from the more recently quoted ι masses of about 1460 MeV.[8] Extracting which wave resonates is much more difficult. It is clear that these data need all three $J^{PG}=0^{-+}$, 1^{++}, and 1^{+-} waves. What is preferred by

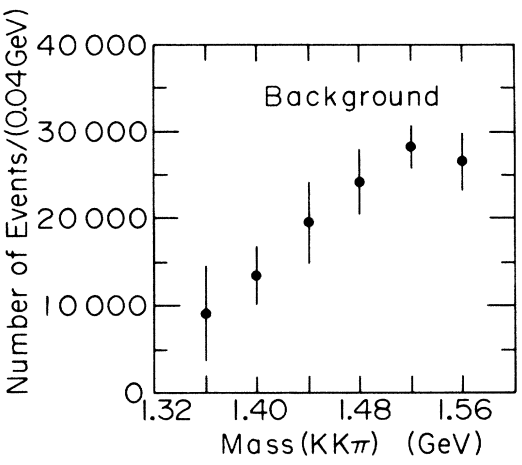

FIG. 11. Acceptance-corrected phase-space background for the best fit.

this analysis is a resonance in the 0^{-+} wave. The possibility of a smaller 1^{++} resonance cannot be excluded by this data. The significance of the resonant 0^{-+} wave decaying into $\delta\pi$ over a flat background is about 3 standard deviations, while the total 0^{-+} wave resonance ($\delta\pi$ and K^*K) is about 2.5 standard deviations. On the other hand, the peak in the 1^{++} wave has a significance of only 1.2 standard deviations and is less than one-fourth the size of the 0^{-+} peak. This analysis also prefers a branching ratio of over 75% for the 0^{-+} wave decaying into $\delta\pi$. The analysis has shown us that is is very important to determine the partial waves of a peak in several mass bins. When the analysis was performed in one mass bin of 100-MeV width, the 1^{++} wave was almost as significant as

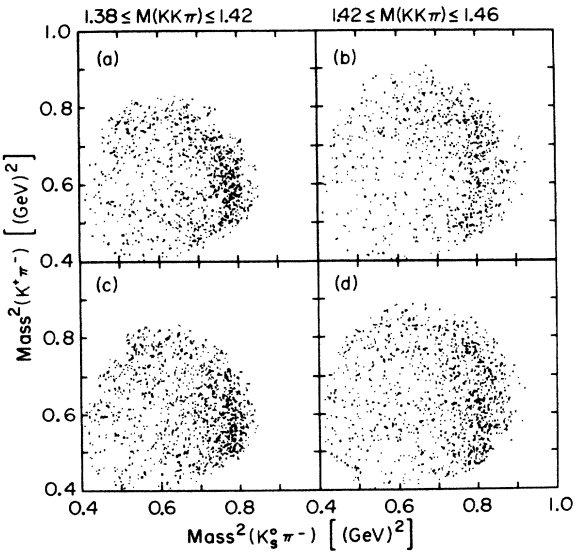

FIG. 12. Dalitz plots of data and Monte Carlo events generated using parameters from the best maximum-likelihood fit. (a) and (b) are data; (c) and (d) are Monte Carlo–simulated events.

the 0^{-+} wave. Also, when we fitted the data in 40-MeV mass bins with just a phase-space background and only one wave, then the 1^{++} wave was preferred over the 0^{-+} wave. Both Dionisi *et al.*[5] and Armstrong *et al.*[7] used one mass bin and conclude that the resonance is 1^{++}, similar to our results. On the other hand, the fit in 40-MeV $K\bar{K}\pi$ mass intervals yields results which are essentially the same as the mass-independent fits of Chung *et al.*[1] of $\pi^- p \to K^+ K_S^0 \pi^- n$ and of Ando *et al.*[6] of $\pi^- p \to \eta\pi\pi n$. Our results are also in agreement with the only other $\bar{p}p$ experiment, that of Baillon *et al.*[4]

In conclusion, these data add more evidence, albeit weak, that the hadronically produced $E(1420)$ is a resonant 0^{-+} wave with a large branching ratio into $\delta\pi$. The data do not exclude a smaller 1^{++} resonance, and in addition require both 1^{++} and 1^{+-} waves to exist. Even though the ι is also most likely a 0^{-+} resonance that decays primarily into $\delta\pi$, the mass and width difference from the E raises the possibility that these are two different resonances.

We gratefully acknowledge the assistance of the alternating-gradient synchrotron crew and the MPS group throughout the experiment, and of J. Albright, P. Meehan, H. Neal, and K. Turner during the run. This research was supported by the U.S. Department of Energy under Contracts No. DE-AC02-76-CH00016, No. DE-AS05-76ER03509, and No. DE-AC02-84ER40125, and by the National Science Foundation under Grant No. PHY-8120739.

[1]S. U. Chung *et al.*, Phys. Rev. Lett. **55**, 779 (1985) (Dalitz-plot analysis); S. U. Chung *et al.*, in *Hadron Spectroscopy—1985,* proceedings of the International Conference, College Park, Maryland, edited by S. Oneda (AIP Conf. Proc. No. 132) (AIP, New York, 1985), p. 27.

[2]R. Armenteros *et al.*, in *Proceedings of the International Conference on Elementary Particle Physics,* Siena, Italy, 1963, edited by G. Bernardini and G. Puppi (Societa Italiana di Fiscia Bologna, Italy, 1963), p. 287.

[3]P. Baillon *et al.*, Nuovo Cimento **50A**, 393 (1967).

[4]P. Baillon, in *Experimental Meson Spectroscopy—1983,* proceedings of the Seventh International Conference, Brookhaven National Laboratory, edited by S. J. Lindenbaum (AIP Conf. Proc. No. 113) (AIP, New York, 1984), p. 78.

[5]C. Dionisi *et al.*, Nucl. Phys. **B169**, 1 (1980).

[6]A. Ando *et al.*, in *Proceedings of the Twelfth International Symposium on Lepton and Photon Interactions at High Energies,* Kyoto, 1985, edited by M. Konuma and K. Takahashi (Nsnissha Printing Co., Kyoto, Japan, 1985).

[7]T. A. Armstrong *et al.*, Phys. Lett. **146B**, 273 (1985).

[8]D. Scharre *et al.*, Phys. Lett. **97B**, 329 (1980); C. Edwards *et al.*, Phys. Rev. Lett. **49**, 259 (1982).

[9]Particle Data Group, Rev. Mod. Phys. **56**, S1 (1984).

[10]S. Protopopescu *et al.*, in *QCD and Beyond,* proceedings of the XXth Rencontre de Moriond, 1985, edited by J. Tran Thanh Van (Editions Frontieres, Gif-sur-Yvette, France, 1985), p. 489; D. Reeves *et al.*, Spin-Parity Analysis of $\bar{p}p \to E(1420)X$, Bull. Am. Phys. Soc. **31**, 878 (1986).

[11]D. F. Reeves, Ph.D. dissertation, Florida State University, 1985.

[12]S. Eiseman *et al.*, Nucl. Instrum. Methods **217**, 140 (1983).

[13]C. Zemach, Phys. Rev. **133**, B1201 (1964).

[14]S. Flatte', Phys. Lett. **63B**, 224 (1976).